PREPRINT

SCIENCE & TECHNOLOGY

Journal homepage: http://www.pertanika.upm.edu.my/

Loss-of-Life Analyses Based on Modified Arrhenius and Relative Aging Rate for Non-Thermally Upgraded Paper in Oil-Immersed Transformer

Najiyah Saleh[1,2], Norhafiz Azis[1,3]*, Jasronita Jasni[1], Mohd Zainal Abidin Ab Kadir[1] and Mohd Aizam Talib[4]

[1]*Advanced Lightning, Power and Energy Research Centre (ALPER), Faculty of Engineering, Universiti Putra Malaysia, 43400 UPM, Serdang, Selangor, Malaysia*
[2]*Electrical Technology Section, Universiti Kuala Lumpur British Malaysian Institute, 53100 Gombak, Selangor, Malaysia*
[3]*Institute of Nanoscience and Nanotechnology (ION2), Faculty of Engineering, Universiti Putra Malaysia, 43400 UPM, Serdang, Selangor, Malaysia*
[4]*TNB Research Sdn Bhd, No. 1, Lorong Ayer Itam, Kawasan Institut Penyelidikan, 43000 Kajang, Selangor, Malaysia*

ABSTRACT

This study evaluates the Loss-of-Life (LOL) based on the modified relative aging rate of an Oil Natural Air Natural (ONAN) transformer with voltage and power ratings of 132/33 kV and 60 MVA. The study's methodology included the determination of the Hotspot Temperature (HST) based on the differential equation in IEC 60076-7. The loading and ambient temperature profiles for HST determination are forecasted based on the Seasonal Autoregressive Integrated Moving Average (SARIMA). Next, a new relative aging rate was developed based on the Arrhenius equation, considering the pre-exponential factors governed by oxygen, moisture in paper, and acids at different content levels. The LOL was computed based on the new relative aging rate. The study's main aim is to examine the impact of pre-exponential factors on the LOL based on modified Arrhenius and relative aging rate. The results indicate that the LOLs for different conditions increase as the oxygen, moisture, low molecular weight acid (LMA), and high molecular weight acid (HMA) increase. The LOLs are 46 days, 1,354 days, and 2,662 days in the presence of 12,000 ppm, 21,000 ppm, and 30,000 ppm of oxygen. In 1%, 3%, and 5%

ARTICLE INFO

Article history:
Received: 28 February 2023
Accepted: 24 August 2023
Published: 14 March 2024

DOI: https://doi.org/10.47836/pjst.32.2.09

E-mail addresses:
najiyahsaleh87@gmail.com (Najiyah Saleh)
norhafiz@upm.edu.my (Norhafiz Azis)
jas@upm.edu.my (Jasronita Jasni)
mzk@upm.edu.my (Mohd Zainal Abidin Ab Kadir)
aizam.talib@tnb.com.my (Mohd Aizam Talib)
* Corresponding author

ISSN: 0128-7680
e-ISSN: 2231-8526

moisture, the LOLs are 477 days, 2,799 days, and 7,315 days. At 1% moisture, the LOL is 1,418 days for LMA, while for HMA, it is 122 days. The LMA has the highest impact on the LOL compared to other aging acceleration factors.

Keywords: Arrhenius equation, cellulose aging, loss-of-life, pre-exponential factor, relative aging rate

INTRODUCTION

It is known that the life of power transformers predominantly relies on cellulose-based insulation. Among the approaches to analyzing the life of cellulose paper insulation is thermal life modeling. This approach determines the hot-spot temperature (HST), insulation paper aging rate, and loss-of-life (LOL) of transformers. The input data of ambient temperature and time-varying load control these parameters. The HST, aging rate, and LOL can be computed through models in international standards.

A sufficient input parameter such as loading and ambient temperature profile is essential to increase the accuracy of HST for assessment of the paper aging rate and LOL. However, in most cases, these parameters are not always available, especially for long intervals. Therefore, forecasting these input data would help with long-term analyses. Several methods to forecast the loading were established by Agrawal et al. (2018), Chen et al. (2017), Hou et al. (2021), Khalid et al. (2020), Khorsheed (2021), Mohammed and Al-Bazi (2022), and Sinha et al. (2021). In addition, the ambient temperature profiles were found in Afzali et al. (2011), Hou et al. (2022), Ma et al. (2020), Radhika and Shashi (2009), Tripathy and Prusty (2021), and Van den Berg et al. (2022). Seasonal Autoregressive Integrated Moving Average (SARIMA) is one of the established methods that can be utilized to forecast any short, medium, or long-term data with the characteristic of strong seasonal patterns and univariate time series (Al-Shaikh et al., 2019). The method is promising for forecasting the future loading and ambient temperature profiles for the transformer's application.

Among the primary contributors to the degradation of insulation paper are temperature and aging acceleration factors, i.e., oxygen, moisture in paper, and acids. Due to non-uniform temperature distribution within a transformer, the region that experiences the highest temperature, referred to as the hot spot, undergoes the most substantial degradation and affects the aging rate of the paper. The modeling of the relative aging rate as per IEC 60076-7 (Feng, 2013; Novkovic et al., 2022) relies mainly on the HST as the important parameter without considering other aging acceleration factors. The model is also applied widely in various studies conducted by Biçen et al. (2011, 2012), Najdenkoski et al. (2007), BL and Mathew (2016) and Piatniczka et al. (2022).

A relative aging rate model that considers several aging acceleration factors was previously examined (Hosseinkhanloo et al., 2022). The relative aging rate is obtained through the ratio of the paper aging rate for any temperatures and conditions over the paper aging rate at the rated condition. The previous study considers two aging factors, i.e., oxygen and moisture, to determine the relative aging rate (Hosseinkhanloo et al., 2022). Recently, the importance of low molecular acid (LMA) and high molecular acid (HMA) to govern paper aging is highlighted, which prompts further modeling study on this aspect. Since the aging in a transformer is a dynamic process, it is anticipated that the pre-exponential factors and activation energies for oxygen and moisture that are directly applied to the CIGRE Brochure 393 (2009) could vary based on the specific aging mechanism to evaluate the relative aging rate.

Modeling paper aging is one of the key aspects of evaluating the integrity of the transformers (Feng, 2013). Currently, there are various methods based on either laboratory accelerated aging experimental data or in-service data that are introduced to evaluate paper aging (Arshad et al., 2004; Liao et al., 2011; Li et al., 2018; Liu et al., 2015; Zhang et al., 2021). The Arrhenius model is one of the common approaches to determining the paper aging rate by considering the aging factors and mechanisms (Feng, 2013). The paper aging rate depends on the HST, pre-exponential factor, and activation energy. Recently, a modified relative aging rate model has been proposed based on the Arrhenius model (Novkovic et al., 2022), which considers the variation of pre-exponential factors according to the paper aging acceleration factors and activation energies, which are based on the aging mechanism (Saleh et al., 2022).

Utilizing the information on pre-exponential factors from the previous work (Saleh et al., 2022), the long-term life assessment based on the modified relative aging rate model is examined. First, the HST is calculated using the differential equation according to IEC 60076-7 (Feng, 2013; Novkovic et al., 2022). The HST computation's loading and ambient temperature profiles are forecasted based on SARIMA. Next, the new relative aging rate is determined based on the pre-exponential factors, the Arrhenius model, and the relative aging rate as per IEC 60076-7 (Feng, 2013; Novkovic et al., 2022). Finally, the LOL is computed based on the pre-determined new relative aging rate. The computation of the new relative aging rate and LOL based on a single aging factor of either oxygen, moisture in paper, or acids in the paper is also examined.

METHODOLOGY

Seasonal Autoregressive Integrated Moving Average (SARIMA)

The forecasting of loading input parameters and ambient temperature profiles was modeled using SARIMA since it supported univariate data with seasonal change. The recorded actual loading profile, taken at 15-minute intervals over 15 days, was utilized to forecast the data for one year. Similar to the loading profile, the ambient temperature profile, recorded at 1-hour intervals for seven months, was used to forecast data for one year.

SARIMA is an enhancement based on the ARIMA model that incorporates the parameters of (p,d,q) × (P,D,Q)m whereby p and P represent the autoregressive and seasonal autoregressive orders, while d and D denote the difference and seasonal difference orders, respectively. Additionally, q and Q indicate the moving averages and seasonal moving average orders, respectively, and m stands for the seasonal period. The SARIMA is expressed by Equation 1 (Cabrera et al., 2013), where each term is mathematically defined as in Equations 2, 3, 4, and 5, respectively.

$$\varphi_P(B)\Phi_p(B^S)\nabla^d\nabla_S^D Z_t = \theta_q(\mathrm{B})\Theta_Q(B^S)a_t \qquad [1]$$

where:

$$\varphi_p(B) = 1 - \varphi_1 B - \varphi_2 B^2 - \cdots - \varphi_p B^p \qquad [2]$$

$$\Phi_P(B^S) = 1 - \Phi_S B^S - \Phi_{2S} B^{2S} - \cdots - \Phi_{PS} B^S \qquad [3]$$

$$\theta_q(B) = 1 - \theta_1 B - \theta_2 B^2 - \cdots - \theta_q B^q \qquad [4]$$

$$\Theta_Q(B^S) = 1 - \Theta_S B^S - \Theta_{2S} B^{2S} - \cdots - \Theta_{QS} B^S \qquad [5]$$

Where p represents the order of non-seasonal auto-regression, d is the number of regular differencing, q denotes the order of non-seasonal MA, P signifies the order of seasonal auto-regression, D is the number of seasonal differencing, Q indicates the order of seasonal MA, S denotes the length of seasonality, φ is the AR operator of order p, Φ is the seasonal AR parameter of order P, d is the differencing operator, D is the seasonal differencing operator, Zt is the observed value at time point t, θ is the MA operator of order q, Θ is the seasonal MA parameter of order Q and a_t is the white noise component of the stochastic model (Cabrera et al., 2013).

Accuracy Measurement

The accuracy measurement of the forecasted loading profile and ambient temperature profile was conducted based on three metrics known as Mean Absolute Percentage Error (MAPE), Mean Absolute Error (MAE), and Root Mean Square Error (RMSE). Low MAPE, MAE, and RMSE indicate a well-fitted model, defined by Equations 6, 7, and 8, respectively.

$$\text{MAPE} = \frac{1}{N}\left(\sum_{t=1}^{N}\left|\frac{Y_t - \hat{Y}_t}{Y_t}\right|\right) \times 100 \qquad [6]$$

$$\text{MAE} = \frac{1}{N}\left(\sum_{t=1}^{N}\left|Y_t - \hat{Y}_t\right|\right) \qquad [7]$$

$$\text{RMSE} = \sqrt{\frac{\sum_{t=1}^{N}(Y_t - \hat{Y}_t)^2}{N}} \qquad [8]$$

Where N is the number of actual data, Y_t is the actual data at time, *t* and $\hat{Y}_t$ is the forecasted data at time, *t*.

Thermal Modelling Parameters

The thermal modeling parameters are essential as the input data to determine a transformer's Top-oil Temperature (TOT) and HST based on the differential equation method. The thermal modeling parameters can typically be obtained from the transformer-specific thermal constants (Susa et al., 2005a; Susa et al., 2005b). The standard thermal modeling parameters can be acquired from IEC 60076-7 without specific thermal constants.

Table 1 shows the thermal modelling parameters for the transformer. The thermal modelling parameters were selected based on the ONAN medium and large power transformers as per IEC 60076-7 (Feng, 2013). The oil time constant, τ_o; winding time constant, τ_w; oil exponent, x; winding exponent, y; the constants, k_{11}, k_{21}, and k_{22}, were acquired as per IEC 60076-7. The ratio of load losses (copper loss) to no-load losses (iron loss), R and top-oil temperature rise at rated current, $\Delta\Theta_{or}$ were obtained per the temperature rise report. The hot-spot to top-oil temperature at rated current, $\Delta\Theta_{hr}$, was calculated based on Equation 9 as per IEC 60076-7 (Feng, 2013; Novkovic et al., 2022; Susa et al., 2005a).

$$\Delta\theta_{hr} = H \times g_r \qquad [9]$$

Where $\Delta\theta_{hr}$ is the hot-spot to top-oil temperature at rated current, *H* is the hot-spot factor while g_r is the average winding to average oil gradient. The value of hot-spot factor, *H* was directly obtained from (Feng, 2013) and the average winding to average oil gradient, g_r was acquired based on the temperature rise report. The time step value, D_3, was set at three minutes since it should be less than half the shortest winding time constant, τ_w as per IEC 60076-7 (Feng, 2013; Novkovic et al., 2022).

Table 1
The thermal modelling parameters

Characteristic	Parameter
Oil exponent, x	0.8
Winding exponent, y	1.3
Constant, k_{11}	0.5
Constant, k_{21}	2.0
Constant, k_{22}	2.0
Oil time constant, τ_o	210
Winding time constant, τ_w	10
Ratio of load losses to no-load losses, R	4.66
Top-oil temperature rise at rated current, $\Delta\Theta_{or}$	44.07
Hot-spot to top-oil temperature at rated current, $\Delta\Theta_{hr}$	33.624
Time step, D_3	3 minutes

Top-Oil Temperature (TOT) and Hot-Spot Temperature (HST) based on IEC60076-7

The TOT and HST were determined based on differential method as per IEC 60076-7 (Feng, 2013; Novkovic et al., 2022). The differential method was selected for its adaptability to the time-varying load and ambient temperature (Feng, 2013). The input parameters of thermal modeling forecasted loading and ambient temperature profiles were utilized to compute the TOT. Subsequently, the HST was computed based on the forecasted loading profile, ambient temperature profile and pre-determined TOT. The evaluation of TOT and HST was considered for a paper's modified relative aging rate.

Relative Aging Rate

According to IEC 60076-7, the HST of 98 °C refers to the aging rate of the transformer's inter-turn insulation under the time and temperature effects for the NTUP (Feng, 2013; Novkovic et al., 2022). Furthermore, the relative aging rate, V was defined based on Equation 10.

$$V = 2^{(\theta_{hst} - 98)/6} \quad [10]$$

Where V is the relative aging rate for NTUP while θ_{hst} is the HST in °C. It is based on Montsigner's life expectancy (Feng, 2013) and Dankin's aging rate formulas (IEEE Standards, 2012), simplified from the Arrhenius equation as shown in Equation 11.

$$\frac{1}{DP_{end}} - \frac{1}{DP_{start}} = Ae^{-\frac{E_a}{R(\theta_{hst}+273)}} \times t \quad [11]$$

Where DP_{end} and DP_{start} are the paper DP at any time, t, or the end-of-life criterion, while DP_{start} is the initial paper DP. On the other hand, A is the pre-exponential factor in 1/h; E_a is the activation energy in kJ/mol, R is the gas constant in 8.314 J/mol/K, θ_{hst} is the HST in °C and t is the lifetime of the insulation in an hour.

Equation 10 implies that the aging rate does not consider different aging factors, i.e., oxygen, moisture, and acids, and it is simply dependent on HST only. The aging rate, k of the insulation paper is given based on Equation 12 (Feng, 2013). The Arrhenius equation assumes that the degradation process of an insulation paper is controlled by the aging rate, k proportional to $exp(-E_a/RT)$.

$$k = Ae^{-\frac{E_a}{RT}} \quad [12]$$

If an aging rate at a certain temperature, as well as the paper aging acceleration factors, are rated as 1.0, then the new relative aging rate, $V_{ntup,modified}$ can be written as Equation 13.

$$V_{ntup,modified} = \frac{\frac{A}{A_r} e^{\frac{1}{R}\left(\frac{E_{a_r}}{\theta_{hst,r}+273} - \frac{Ea}{\theta_{hst}+273}\right)}}{2^{(\theta_{hst}-98)/6}} \quad [13]$$

where $V_{ntup,modified}$ is the new relative aging rate for NTUP, and the subscript r represents the rated condition. The rated relative aging rate $V = 1.0$, at this condition, was set according to the IEC 60076-7 approach (Feng, 2013; Novkovic et al., 2022), which corresponds to a temperature of 98 °C for NTUP (CIGRE Brochure 738, 2018).

The flow chart of the modified relative aging rate based on aging factors is shown in Figure 1. The first step was to obtain the data of HST, θ_{hst} based on the differential equation method in IEC 60076-7. Next, the rated condition of activation energy, E_{a_r} was determined based on the maximum activation energy variation (Ese et al., 2010; Teymouri & Vahidi, 2019; Lundgaard et al., 2008). The rated pre-exponential factor, A_r was obtained from Saleh et al. (2022) based on the maximum aging factors condition. The activation energy, E_a for each of the aging mechanisms was set based on Ese et al. (2010) for oxidation, while the values for hydrolysis and acid-catalyzed hydrolysis were set based on the average activation energies from Teymouri and Vahidi (2019) and Lundgaard et al. (2008), respectively.

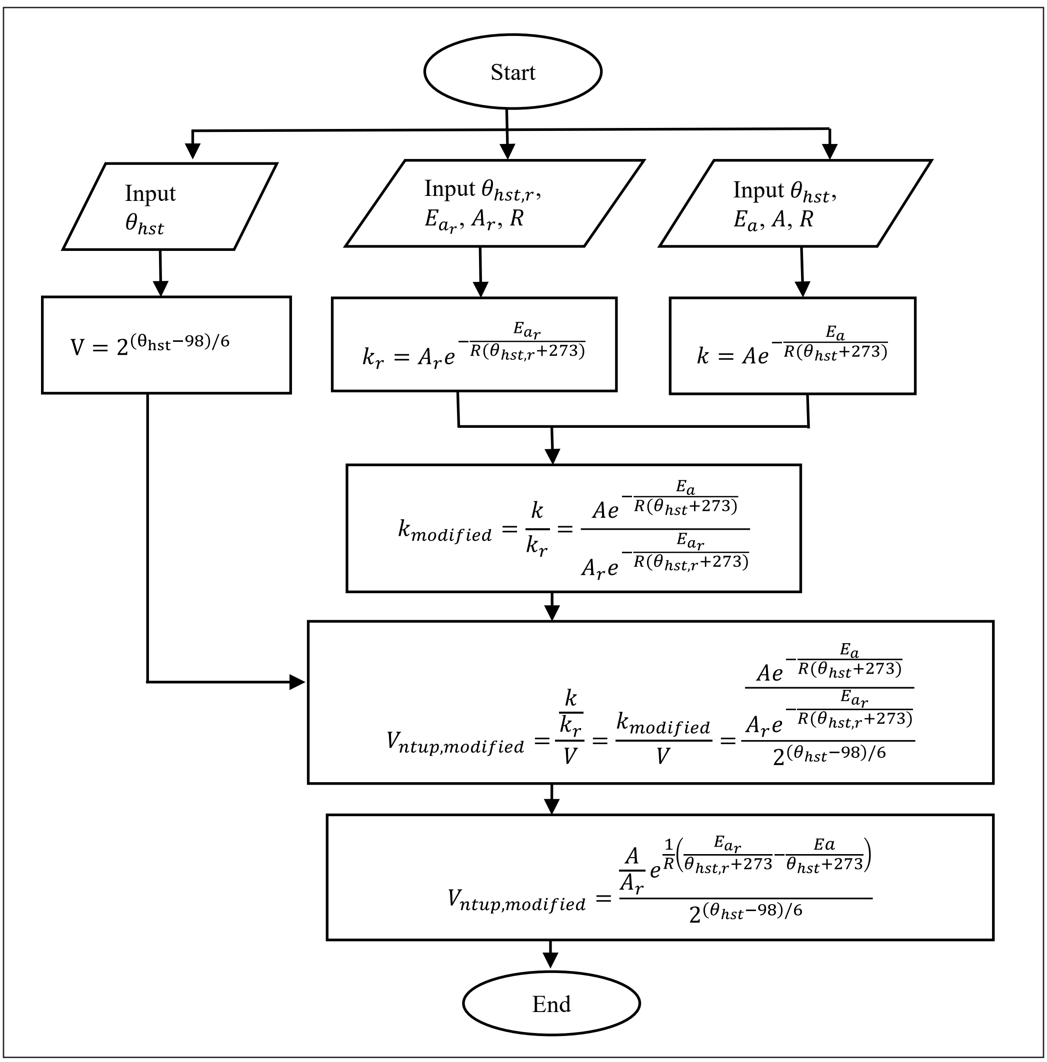

Figure 1. The flow chart of modified relative aging rate based on the aging factors

Similarly, the pre-exponential factor, A was obtained from Saleh et al. (2022) and relied on the types and concentrations of aging factors. All inputs were applied to the formula of the relative aging rate as per IEC 60076-7 (Feng, 2013; Novkovic et al., 2022), the aging rate under the effects of aging factors, k and the rated condition of the aging rate, k_r. The aging rate according to the oxygen, moisture and acids, $k_{modified}$ was determined based on the ratio of k and k_r (Hosseinkhanloo et al., 2022; Novkovic et al., 2022). The modified relative aging rate with temperature, oxygen, moisture and acids content as a controlling parameter, $V_{ntup,modified}$ is the ratio between $k_{modified}$ and V.

Loss-of-Life (LOL)

The loss-of-life, L over a certain period is given by Equation 14.

$$L = \int_{t_1}^{t_2} V_{ntup\,,modified}\ dt \text{ or } L \approx \sum_{n=1}^{N} V_{ntup\,,modified}\ t_n \qquad [14]$$

where $V_{ntup,modified}$ is the relative aging rate during interval according to Equation 13, t_n is the nth time interval, n is the number of each time interval, and N is the total number of intervals during the period.

RESULTS AND ANALYSIS

Forecasting of Transformer Loading and Ambient Temperature Profile

The loading profile of an ONAN transformer with voltage and power ratings of 132/33 kV and 60 MVA is shown in Figure 2. The actual loading profile was obtained based on the interval of 15 minutes for a duration of up to 15 days. Next, the loading profile was forecasted up to 24 steps to obtain one year of data. The accuracy measurement based on MAPE, MAE, and RMSE was utilized to determine the best SARIMA model for each

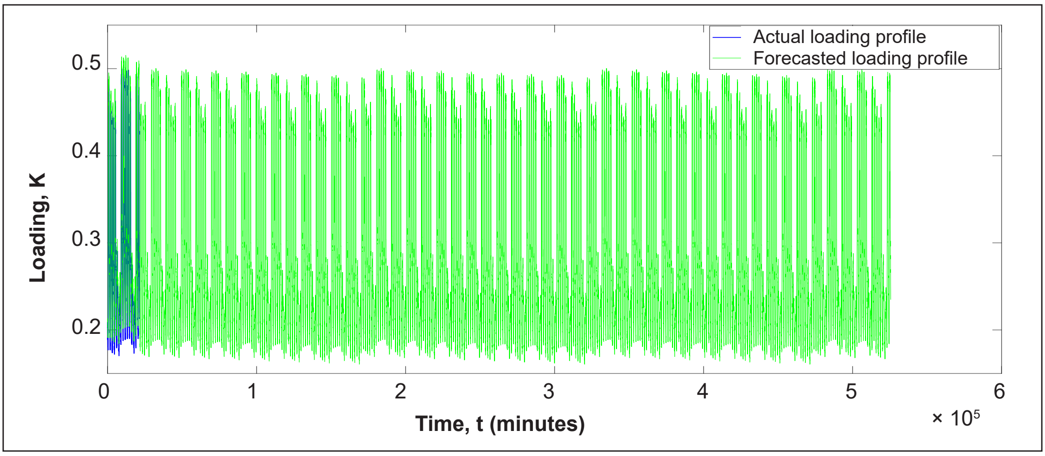

Figure 2. The loading profile of the ONAN transformer for one year

predicted loading profile, as seen in Table 2 (Saleh et al., 2021). MAPE, MAE and RMSE indicate the errors between the actual and forecasted data. The forecasted loading profile, validated by comparison with the actual loading profile, shows that the MAPE, MAE, and RMSE are less than 10% (Saleh et al., 2021).

Table 2
The best mode of the SARIMA model for forecasted loading profile

Forecasting	Model (p,d,q)x(P,D,Q)$_{672}$	MAPE	MAE	RMSE
1-step ahead	010×110	0.1376	0.0375	0.0788
2-steps ahead	112×110	0.2206	0.0643	0.1089
3-steps ahead	112×110	0.2219	0.0657	0.1090
4-steps ahead	112×110	0.2368	0.0725	0.1145
5-steps ahead	112×110	0.2405	0.0746	0.1172
6-steps ahead	112×110	0.1421	0.0445	0.0809
7-steps ahead	112×110	0.0611	0.0183	0.0254
8-steps ahead	010×110	0.1376	0.0375	0.0788
9-steps ahead	112×110	0.2206	0.0643	0.1089
10-steps ahead	112×110	0.2219	0.0657	0.1090
11-steps ahead	112×110	0.2368	0.0725	0.1145
12-steps ahead	112×110	0.2405	0.0746	0.1172
13-steps ahead	112×110	0.1421	0.0445	0.0809
14-steps ahead	112×110	0.0611	0.0183	0.0254
15-steps ahead	010×110	0.1376	0.0375	0.0788
16-steps ahead	112×110	0.2206	0.0643	0.1089
17-steps ahead	112×110	0.2219	0.0657	0.1090
18-steps ahead	112×110	0.2368	0.0725	0.1145
19-steps ahead	112×110	0.2405	0.0746	0.1172
20-steps ahead	112×110	0.1421	0.0445	0.0809
21-steps ahead	112×110	0.0611	0.0183	0.0254
22-steps ahead	010×110	0.1376	0.0375	0.0788
23-steps ahead	112×110	0.2206	0.0643	0.1089
24-steps ahead	112×110	0.2033	0.0669	0.1058

Figure 3 shows the ambient temperature profile recorded at one-hour intervals for seven months. The best modes of the SARIMA model for each forecasted ambient temperature profile are shown in Table 3. The comparison between the forecasted and the actual ambient temperature profiles based on the MAPE, MAE, and RMSE are below 10%, signifying a high level of accuracy.

Top-Oil Temperature (TOT) and Hot-Spot Temperature (HST)

The TOT profile based on the predicted ambient temperature profile and loading profile is depicted in Figure 4. The highest value of TOT is 54.6°C, while the lowest TOT is 36°C.

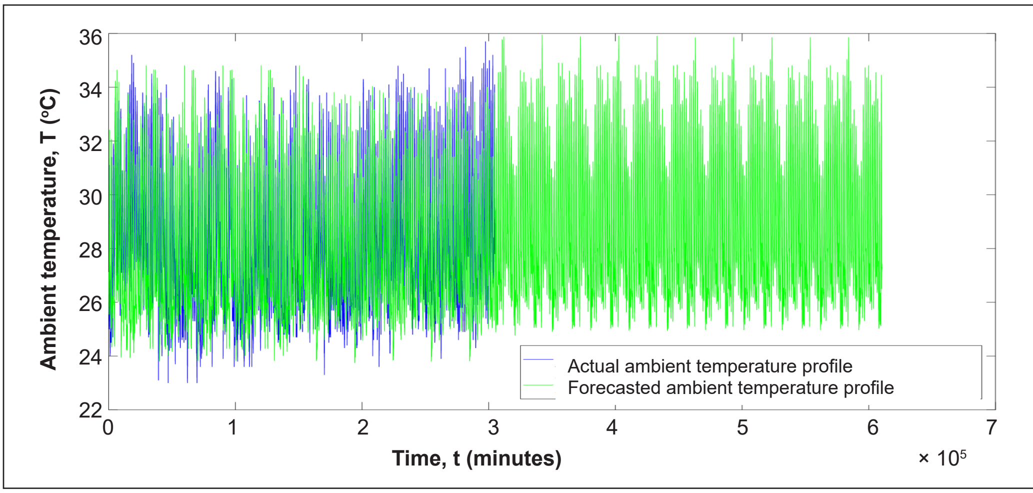

Figure 3. The ambient temperature profile of ONAN transformer for one year

Table 3
The best mode of the SARIMA model for forecasted ambient temperature profile

Forecasting	Model $(p,d,q)x(P,D,Q)_{168}$	MAPE	MAE	RMSE
1-step ahead	000×231	0.0607	1.6778	2.3417
2-steps ahead	000×132	0.0512	1.4447	2.0065

Note. For each 1-step ahead of forecasting, it is equal to 3.5 months or 14 weeks

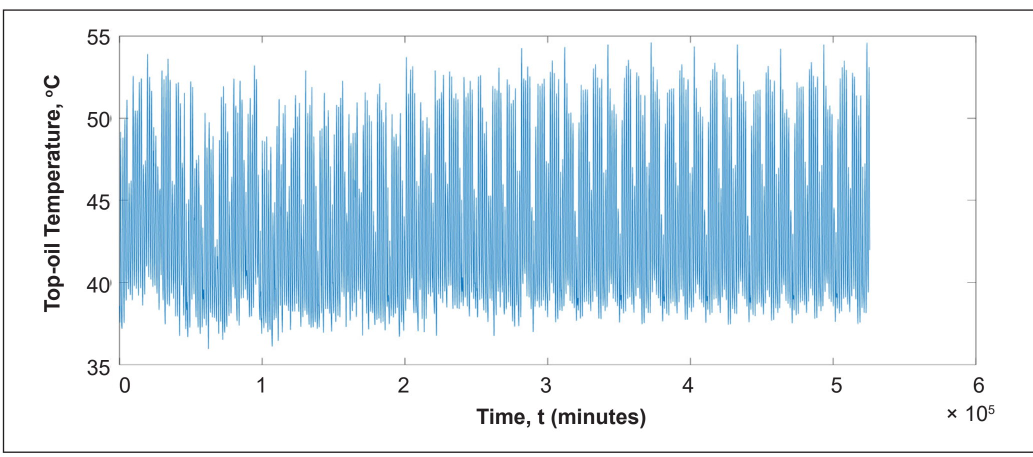

Figure 4. The TOT profile of ONAN transformer for one year

The average TOT is 43.2°C. The HST was computed based on the forecasted loading profile, ambient temperature profile and TOT shown in Figure 5. The highest predicted HST is 68.1°C, whereas the lowest HST is 39.5°C. The average HST is 50.2°C for one year.

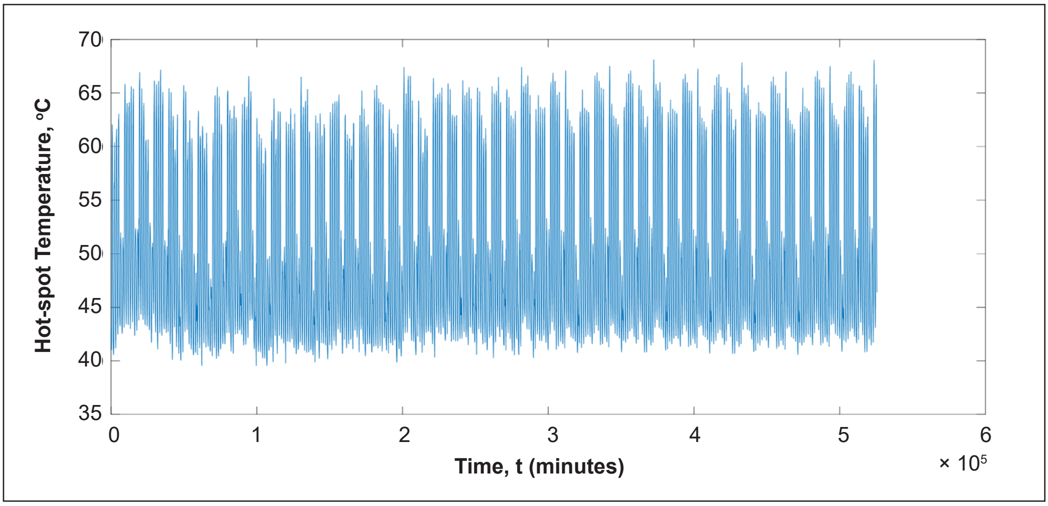

Figure 5. The HST profile of the ONAN transformer for one year

Loss-of-Life (LOL) with Different Oxygen Concentrations

The relative aging rate of a transformer at different oxygen concentrations and moisture in paper less than 0.5% is shown in Figures 6(a) to 6(c). The corresponding pre-exponential factor was obtained for each oxygen concentration (Saleh et al., 2022). The activation energy was 74 kJ/mol, while the oxygen concentration was varied. The rated pre-exponential factor was set once

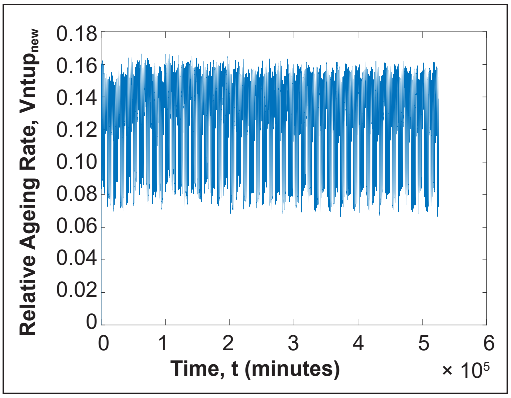

(a)

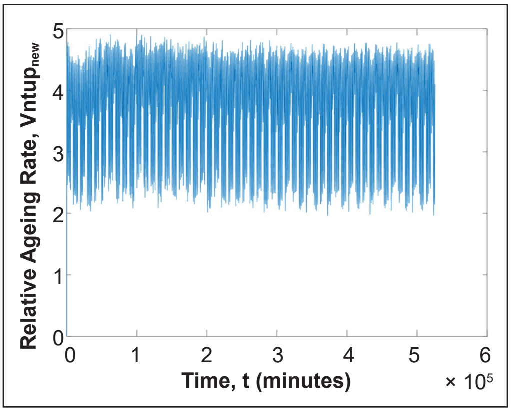

(b)

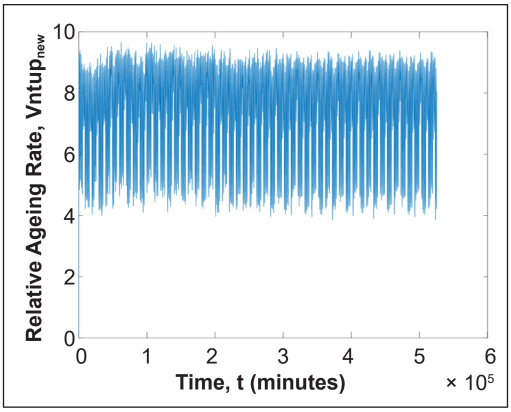

(c)

Figure 6. The relative aging rate of a transformer at moisture less than 0.5% under oxygen concentration of (a) 12,000 ppm, (b) 21,000 ppm, and (c) 30,000 ppm

the oxygen concentration of 30,000 ppm was reached (CIGRE Brochure 738, 2018). The increment of oxygen concentration causes the average and highest relative aging rate to increase linearly (Table 4).

Table 4
The average and highest relative aging rate of a transformer at different oxygen concentrations and moisture less than 0.5%

Oxygen concentration, P (ppm)	Average relative ageing rate	Highest relative ageing rate
12,000	0.1259	0.1665
21,000	3.7094	4.9082
30,000	7.2929	9.6500

For each of the increasing steps, The LOL at different oxygen concentrations and moisture in paper less than 0.5% exponentially increases with time, as shown in Figures 7(a) to 7(c). The increment of oxygen concentration from 12,000 ppm to 21,000 ppm causes the LOL to increase by 29.5 (Table 5). The LOL factor increases to two when the oxygen concentration increases from 21,000 ppm to 30,000 ppm. Overall, the oxygen concentration increments from 12,000 ppm to 30,000 ppm, incrementing the LOL factor by 57.9.

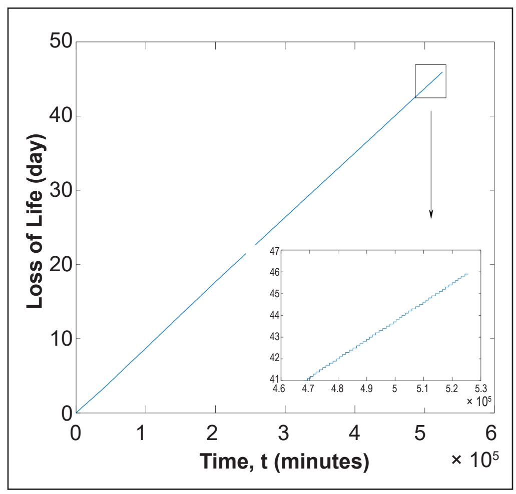

(a)

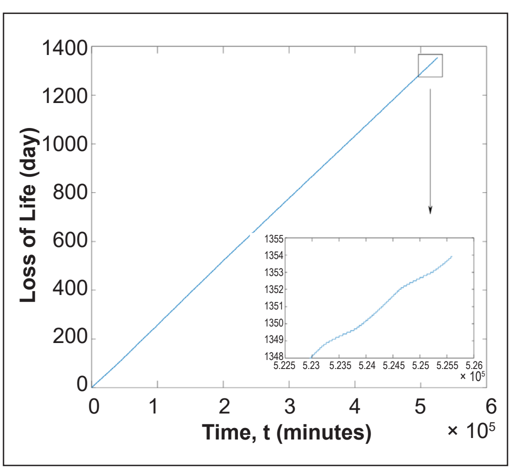

(b)

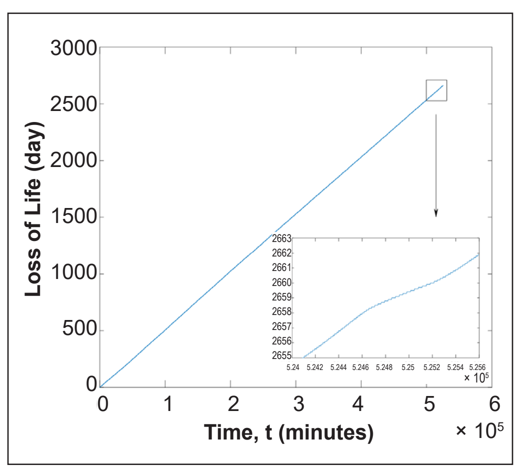

(c)

Figure 7. The LOL of a transformer at moisture less than 0.5% under oxygen concentration of (a) 12,000 ppm, (b) 21,000 ppm, and (c) 30,000 ppm

Table 5
The accumulated LOL value for a transformer at different oxygen concentrations and moisture less than 0.5%

Oxygen concentration, P (ppm)	Loss-of-Life (minutes)	Loss-of-Life (days)	Loss-of-Life (years)
12,000	6.6152×10^4	45.9392	≈ 0.1
21,000	1.9496×10^6	1.3539×10^3	≈ 4
30,000	3.8331×10^6	2.6619×10^3	≈ 7

Loss-of-Life (LOL) with Different Moisture Contents

The pre-exponential factors for the moisture in the paper of 1%, 3%, and 5% were utilized based on Saleh et al. (2022) to determine the relative aging rate of a transformer. The factor was determined based on the low oxygen concentration, i.e., less than 7,000 ppm. The transformer's relative aging rate at various moisture contents under low oxygen concentration is depicted in Figures 8(a) to 8(c). The activation energy for different moisture content was set to 120 kJ/mol, while the rated activation energy was set to 130 kJ/mol since it represents a hydrolysis aging mechanism (Teymouri & Vahidi, 2019). The moisture content of the rated pre-exponential factor was 5.0%, indicating wet conditions (Arshad & Islam, 2011). The average and highest relative aging rate increases approximately linear once there is an increment of moisture content in the paper (Table 6).

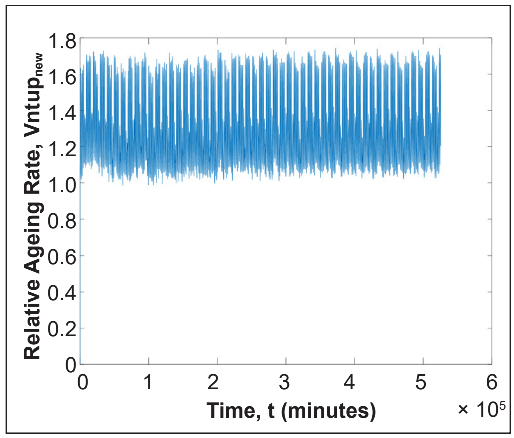

(a)

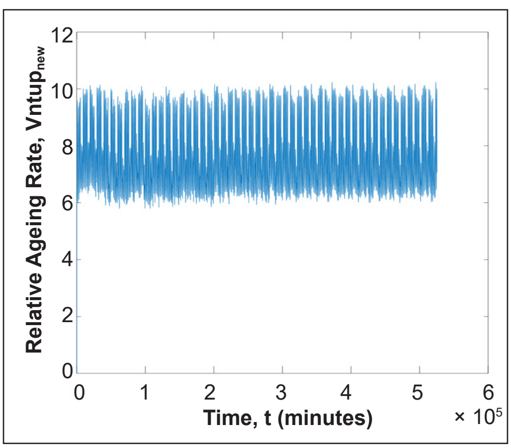

(b)

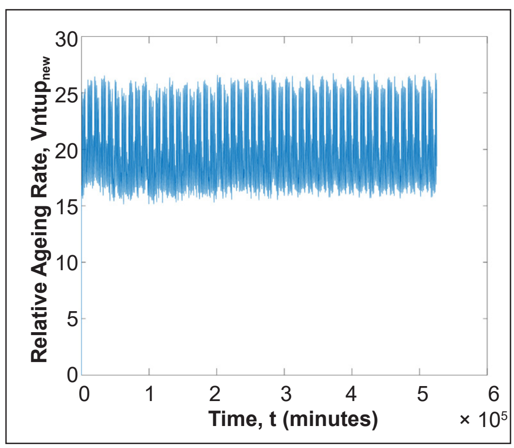

(c)

Figure 8. The relative aging rate of a transformer at low oxygen concentration under moisture content of (a) 1.0%, (b) 3.0%, and (c) 5.0%

Table 6
The average and highest relative aging rate of a transformer at various moisture content under a low oxygen concentration

Moisture content, w (%)	Average relative aging rate	Highest relative aging rate
1.0	1.3058	1.7423
3.0	7.6677	10.2307
5.0	20.0407	26.7394

The LOL of a transformer at various moisture content in the paper under low oxygen concentrations is shown in Figure 9(a) to (c). The LOL of a transformer increases over one year once the moisture content increases from 1.0% to 5.0%. The LOL increases exponentially with time for each of the increasing step intervals. The increment of moisture content from 1% to 3% causes the LOL to increase by 5.9 (Table 7). The LOL factor increases further by 2.6 once

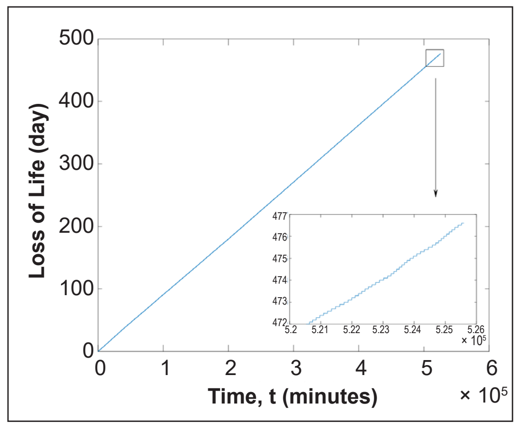

(a)

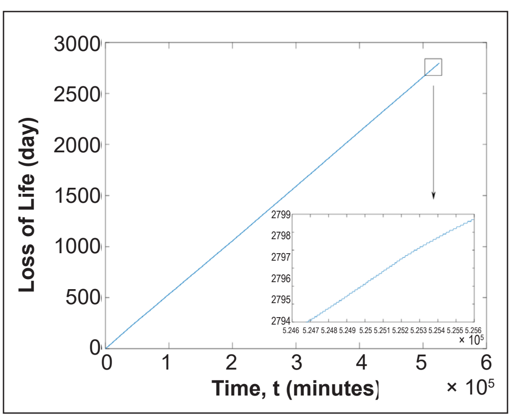

(b)

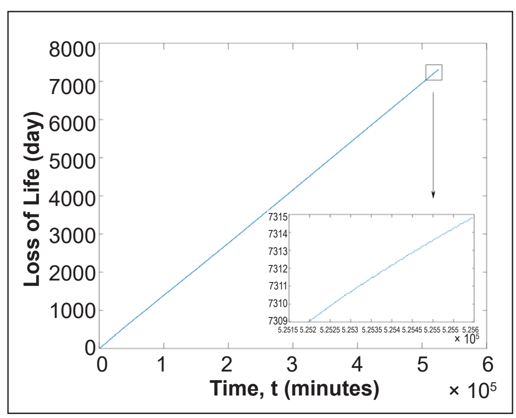

(c)

Figure 9. The LOL of a transformer at low oxygen concentration under moisture content of (a) 1.0%, (b) 3.0%, and (c) 5.0%

Table 7
The accumulated LOL value for a transformer at various moisture content under low oxygen concentration

Moisture content, w (%)	Loss-of-Life (minutes)	Loss-of-Life (days)	Loss-of-Life (years)
1.0	6.8633×10^5	476.6153	≈ 1
3.0	4.0302×10^6	2.7987×10^3	≈ 8
5.0	1.0533×10^7	7.3148×10^3	≈ 20

the moisture content increases from 3% to 5%. The LOL factor increases by 15.3 once the moisture content increases from 1% to 5%.

Loss-of-Life (LOL) with Acids

The pre-exponential factors for LMA and HMA were obtained based on Saleh et al. (2022). These factors were chosen at a moisture content of 1% for both acids while the activation energy was 95 kJ/mol. The pre-exponential factor of LMA at 5% of moisture content was used for the rated condition. The rated activation energy was set to 105 kJ/mol. The relative aging rate for a transformer under LMA and HMA with 1% moisture content can be observed in Figures 10 and 11, respectively. The recorded average and highest relative aging rate for a transformer under LMA and HMA at 1% of moisture content is shown in Table 8. The HMA has a lower average and highest relative aging rates as compared to the LMA.

The LOL of a transformer under LMA and HMA at 1% of moisture content are shown in Figures 12 and 13. The LOL of a transformer under LMA is high, and it can cause a higher impact on paper degradation as compared to the HMA. The LOL rises exponentially with increasing step intervals over one year. The LOL increases by a factor of 11.6 for LMA relative to the HMA at a moisture content of 1% (Table 9).

Table 8
The average and highest relative aging rate for a transformer under LMA and HMA at 1% of moisture content

Moisture content, w (%)	Type of acids	Average relative aging rate	Highest relative aging rate
1.0	LMA	3.8858	4.0635
	HMA	0.3352	0.3505

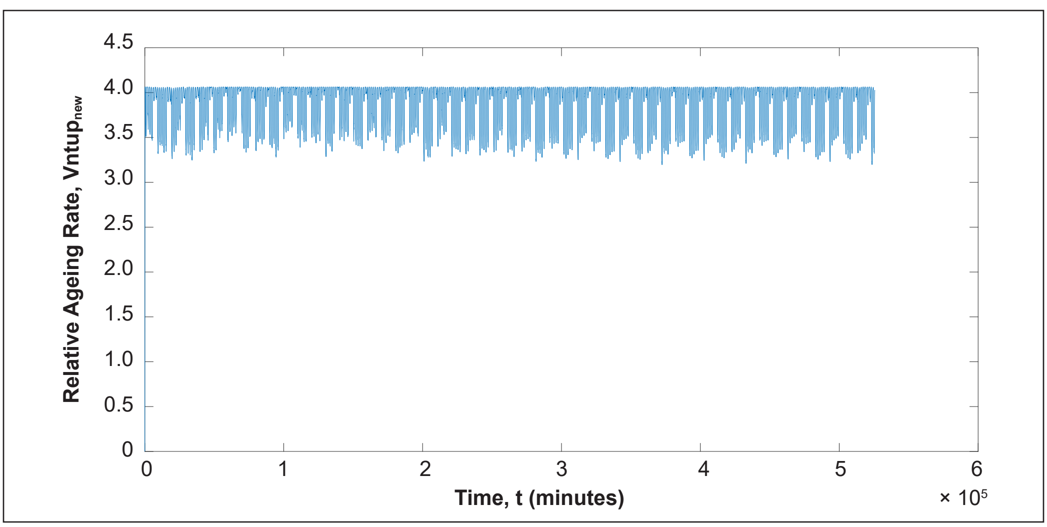

Figure 10. The relative aging rate of a transformer under LMA at the moisture content of 1%

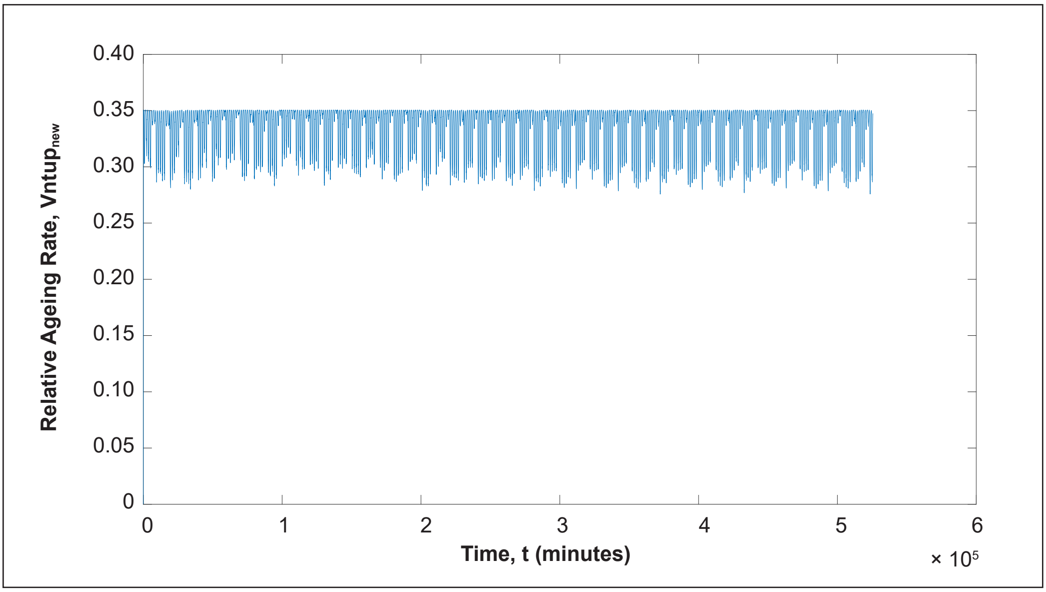

Figure 11. The relative aging rate of a transformer under HMA at the moisture content of 1%

Table 9
The accumulated LOL of a transformer under LMA and HMA at the moisture of 1%

Moisture content, w (%)	Type of acids	Loss-of-Life (minutes)	Loss-of-Life (days)	Loss-of-Life (years)
1.0	LMA	2.0424×10^6	1418.3241	≈ 4
	HMA	1.7616×10^5	122.3365	≈ 0.3

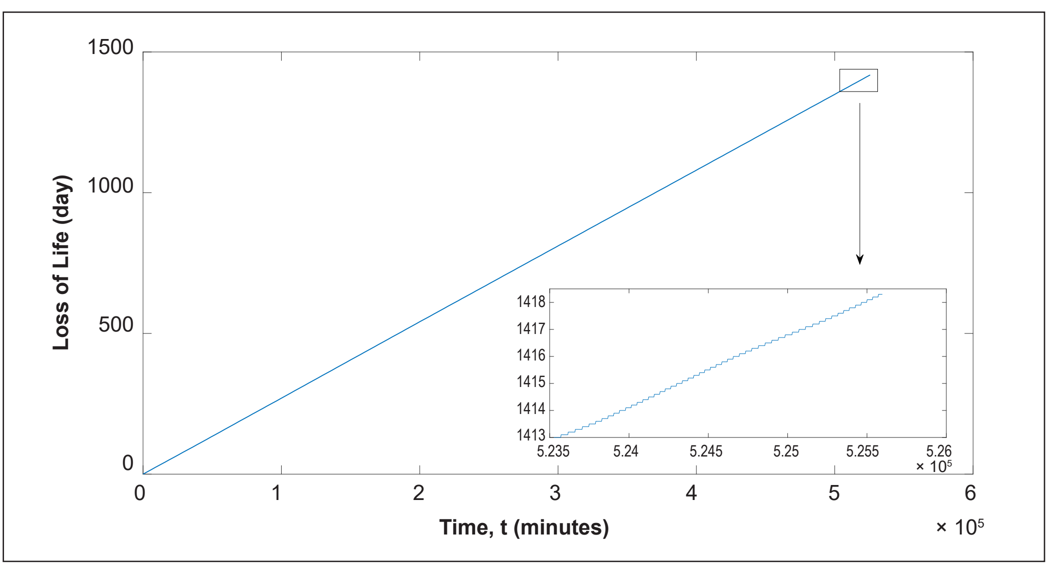

Figure 12. The LOL of a transformer under LMA at the moisture content of 1%

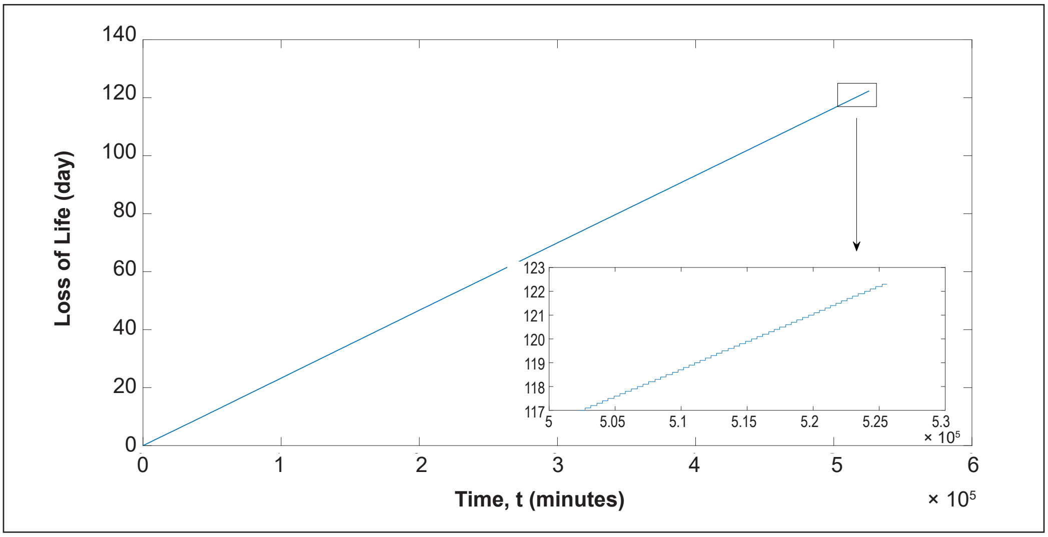

Figure 13. The LOL of a transformer under HMA at the moisture content of 1%

DISCUSSION

Based on the current study, the LOL under the effects of oxygen, moisture, LMA and HMA increases exponentially throughout one year of duration. The LOL increases linearly due to the small range between each time step and the large range between the initial and final computations. The LOL under LMA gives the most impact compared to another factor since it is known to react together with moisture to enhance the hydrolysis mechanism (CIGRE Brochure 323, 2007; Lundgaard et al., 2008). The increment of oxygen concentration up to 1,000 ppm can cause the LOL of a transformer to increase by factors between one and four.

The increment of moisture content in paper to 0.5% can cause an increment of LOL by factors between one and two. As the oxygen concentration and moisture content increase, the factor decreases. The decreasing factor means that the transformer's life will continue to gradually decline until it reaches zero, which means the transformer is at the very end of its life and can no longer be used. For an NTUP, it is obvious that the moisture can cause a higher impact on the transformer's LOL as compared to the oxygen (CIGRE Brochure 323, 2007; Hosseinkhanloo et al., 2022). It is apparent that the assessment of transformer LOL depends not only on the loading, ambient temperature, and HST but also on the aging factor and mechanism reaction of a transformer.

The comparison of LOL based on different effects of the aging factor for a transformer can be seen in Figure 14. The LOL, for one year of duration based on temperature is the lowest, at only two days. In contrast, the LOL under moisture content of 5% at low oxygen concentration gives the highest LOL for one year. The factor of LOL is 20.5 for 12,000 ppm of oxygen concentration relative to the function of temperature at moisture less than

0.5%. The oxygen concentration of 21,000 ppm and 30,000 ppm relative to the function of temperature yields the factor of 602.8 and 1185.2. The factors of LOL at 1%, 3%, and 5% of moisture content relative to the function of temperature under low oxygen concentration are 212.2, 1246.1, and 3256.8. The factor of LOL for LMA with regard to the temperature at 1% of moisture content is 631.5. On the other hand, the LOL factor for HMA relative to the function of temperature at 1% of moisture content is 54.5. Based on Figure 14, LMA at 1% moisture content results in higher LOL for the one-year duration compared to LOL under 1% moisture content at low oxygen concentration.

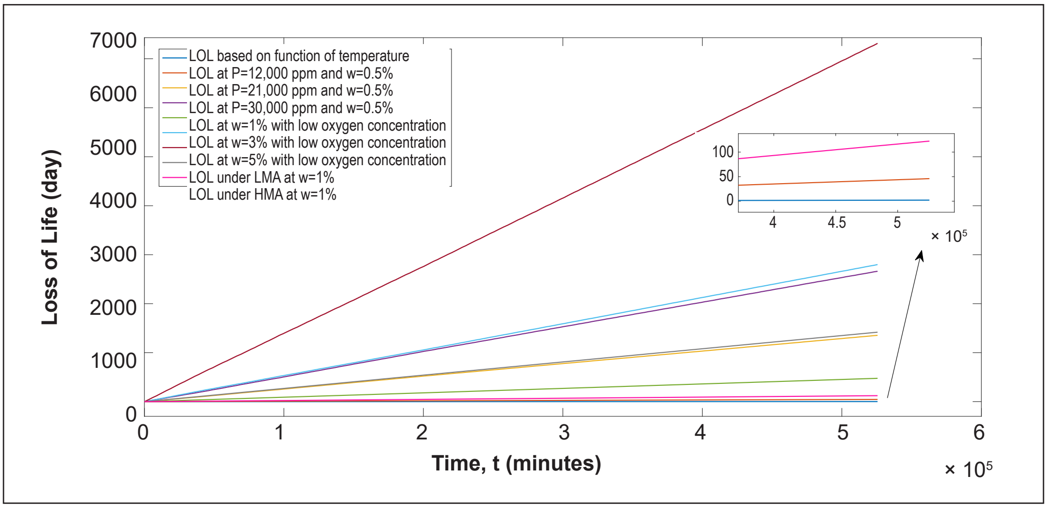

Figure 14. The comparison of LOL based on different effects of the aging factor

CONCLUSION

It is apparent that with the newly developed relative aging rate, the LMA has the most significant impact on the transformer's LOL, followed by moisture, oxygen, and HMA. Based on the current study, the LOL increases with increasing oxygen concentration from 12,000 ppm to 30,000 ppm. The increment of moisture content from 0.5% to 5% also increases the LOL of a transformer. The LOL of a transformer increases exponentially with time for each increasing step interval regardless of the presence of any aging factors. LMA has a higher impact than HMA, leading to 1,418 days of LOL compared to 122 days of LOL. The transformer's LOL in days increases proportionally in the presence of oxygen concentration and moisture content. The impact of oxygen on a transformer's LOL is low compared to moisture and LMA for the NTUP.

ACKNOWLEDGEMENTS

The authors would like to thank the Ministry of Higher Education Malaysia, for funding the study under the FRGS scheme of FRGS/1/2019/TK07/UPM/02/3 (03-01-19-2071FR).

REFERENCES

Afzali, M., Afzali, A., & Zahedi, G. (2011). Ambient air temperature forecasting using artificial neural network approach. In *2011 International Conference on Environmental and Computer Science IPCBEE* (Vol.19, pp. 176-180). IACSIT Press.

Agrawal, R. K., Muchahary, F., & Tripathi, M. M. (2018). Long term load forecasting with hourly predictions based on long-short-term-memory networks. In *2018 IEEE Texas Power and Energy Conference (TPEC)* (pp. 1-6). IEEE Publishing. https://doi.org/10.1109/TPEC.2018.8312088

Al-Shaikh, H., Rahman, M. A., & Zubair, A. (2019). Short-term electric demand forecasting for power systems using similar months approach based SARIMA. In *2019 IEEE International Conference on Power, Electrical, and Electronics and Industrial Applications (PEEIACON)* (pp. 122-126). IEEE Publishing. https://doi.org/10.1109/PEEIACON48840.2019.9071939

Arshad, M., & Islam, S. M. (2011). Significance of cellulose power transformer condition assessment. *IEEE Transactions on Dielectrics and Electrical Insulation, 18*(5), 1591-1598. https://doi.org/10.1109/TDEI.2011.6032829

Arshad, M., Islam, S. M., & Khaliq, A. (2004). Power transformer aging and life extension. In *8th International Conference on Probabilistic Methods Applied to Power Systems* (pp. 498-501). IEEE Publishing.

Biçen, Y., Çilliyüz Y., Aras, F. & Aydugan, G. (2012). Aging of paper insulation in natural ester & mineral oil. *Electrical and Electronic Engineering, 2*(3), 141-146. https://doi.org/10.5923/j.eee.20120203.06

Biçen, Y., Çilliyüz, Y., Aras, F., & Aydugan, G. (2011). An assessment on aging model of IEEE/IEC standards for natural and mineral oil-immersed transformer. In *2011 IEEE International Conference on Dielectric Liquids* (pp 1-4). IEEE Publishing. https://doi.org/10.1109/ICDL.2011.6015442

Kumar, B. L. P., & Mathew, R. (2016). Asset management of transformer based on loss of life calculation. In *2016 IEEE 6th International Conference on Power Systems (ICPS)* (pp. 1-5). IEEE Publishing. https://doi.org/10.1109/ICPES.2016.7584000

Cabrera, N. G., Gutiérrez-Alcaraz, G., & Gil, E. (2013). Load forecasting assessment using SARIMA model and fuzzy inductive reasoning. In *2013 IEEE International Conference on Industrial Engineering and Engineering Management* (pp. 561-565). IEEE Publishing. https://doi.org/10.1109/IEEM.2013.6962474

Chen, Y., Xu, P., Chu, Y., Li, W., Wu, Y., Ni, L., Bao, Y., & Wang, K. (2017). Short-term electrical load forecasting using the support vector regression (SVR) model to calculate the demand response baseline for office buildings. *Applied Energy, 195*, 659-670. https://doi.org/10.1016/j.apenergy.2017.03.034

CIGRE Brochure 323. (2007). Ageing of cellulose in mineral-oil insulated transformers. In *D1 Materials and Emerging Test Techniques*. CIGRE. https://www.e-cigre.org/publications/detail/323-ageing-of-cellulose-in-mineral-oil-insulated-transformers.html,

CIGRE Brochure 393. (2009). Thermal performance of transformers. In *A2 Power Transformers and Reactors.* CIGRE. https://www.e-cigre.org/publications/detail/393-thermal-performance-of-transformers.html

CIGRE Brochure 738. (2018). Ageing of liquid impregnated cellulose for power transformers. In *D1 Materials and Emerging Test Techniques*. CIGRE. https://www.e-cigre.org/publications/detail/738-ageing-of-liquid-impregnated-cellulose-for-power-transformers.html

Ese, M. H. G., Liland, K. B., & Lundgaard, L. E. (2010). Oxidation of paper insulation in transformers. *IEEE Transactions on Dielectrics and Electrical Insulation, 17*(3), 939-946. https://doi.org/10.1109/TDEI.2010.5492270

Feng, D. (2013). *Life Expectancy Investigation of Transmission Power Transformers* (Doctoral dissertation). The University of Manchester, England. https://www.escholar.manchester.ac.uk/api/datastream?publicationPid=uk-ac-man-scw:187566&datastreamId=FULL-TEXT.PDF

Hosseinkhanloo, M., Kalantari, N. T., Behjat, V., & Ravadanegh, S. N. (2022). Optimal exploitation of power transformer fleet considering loss of life and economic evaluation based on failure probability. *Electric Power Systems Research, 213*, Article 108801. https://doi.org/10.1016/j.epsr.2022.108801

Hou, J., Wang, Y., Zhou, J., & Tian, Q. (2022). Prediction of hourly air temperature based on CNN-LSTM. *Geomatics, Natural Hazards and Risk, 13*(1), 1962-1986. https://doi.org/10.1080/19475705.2022.2102942

Hou, T., Fang, R., Tang, J., Ge, G., Yang, D., Liu, J., & Zhang, W. (2021). A novel short-term residential electric load forecasting method based on adaptive load aggregation and deep learning algorithms. *Energies, 14*(22), Article 7820. https://doi.org/10.3390/en14227820

Khalid, R., Javaid, N., Al-zahrani, F. A., Aurangzeb, K., Qazi, E. U. H., & Ashfaq, T. (2020). Electricity load and price forecasting using Jaya-Long Short Term Memory (JLSTM) in smart grids. *Entropy, 22*, Article 10. https://doi.org/10.3390/e22010010

Khorsheed, E. (2021). Energy load forecasting: Bayesian and exponential smoothing hybrid methodology. *International Journal of Energy Sector Management, 15*(2), 294-308. https://doi.org/10.1108/IJESM-06-2019-0005

Li, J., Zhang, J., Wang, F., Huang, Z., & Zhou, Q. (2018). A novel aging indicator of transformer paper insulation based on dispersion staining colors of cellulose fibers in oil. *IEEE Electrical Insulation Magazine, 34*(4), 8-16. https://doi.org/10.1109/MEI.2018.8430039

Liao, R. J., Yang, L. J., Li, J., & Grzybowski, S. (2011). Aging condition assessment of transformer oil-paper insulation model based on partial discharge analysis. *IEEE Transactions on Dielectrics and Electrical Insulation, 18*(1), 303-311. https://doi.org/10.1109/TDEI.2011.5704522

Liu, J., Liao, R., Zhang, Y., Gong, C., Wang, C., & Gao, J. (2015). Condition evaluation for aging state of transformer oil-paper insulation based on time-frequency domain dielectric characteristics. *Electric Power Components and Systems, 43*(7), 759-769. https://doi.org/10.1080/15325008.2014.991462

Lundgaard, L. E., Hansen, W., & Ingebrigtsen, S. (2008). Ageing of mineral oil impregnated cellulose by acid catalysis. *IEEE Transactions on Dielectrics and Electrical Insulation, 15*(2), 540-546. https://doi.org/10.1109/TDEI.2008.4483475

Ma, X., Fang, C., & Ji, J. (2020). Prediction of outdoor air temperature and humidity using Xgboost. *IOP Conference Series: Earth and Environmental Science, 427*, Article 012013. https://doi.org/10.1088/1755-1315/427/1/012013

Mohammed, N. A., & Al-Bazi, A. (2022). An adaptive backpropagation algorithm for long-term electricity load forecasting. *Neural Computing and Applications, 34*, 477-491. https://doi.org/10.1007/s00521-021-06384-x

Najdenkoski, K., Rafajlovski, G., & Dimcev, V. (2007). Thermal aging of distribution transformers according to IEEE and IEC standards. In *2007 IEEE Power Engineering Society General Meeting* (pp. 1-5). IEEE Publishing. https://doi.org/10.1109/PES.2007.385642

Novkovic, M., Popovic, A., Briosso, E., Iglesias, R. M., & Radakovic, Z. (2022). Dynamic thermal model of liquid-immersed shell-type transformers. *International Journal of Electrical Power & Energy Systems, 142*, Article 108347. https://doi.org/10.1016/j.ijepes.2022.108347

Piatniczka, A., Kockott, M., Bistaffa, G., & Paduraru, S. (2022). Transformer loss of life monitoring: A review of in-service highlighting achieved benefits. In *2022 75th Annual Conference for Protective Relay Engineers (CPRE)* (pp. 1-7). IEEE Publishing. https://doi.org/10.1109/CPRE55809.2022.9776562

Radhika, Y., & Shashi, M. (2009). Atmospheric temperature prediction using support vector machines. *International Journal of Computer Theory and Engineering, 1*(1), 55-58. https://doi.org/10.7763/ijcte.2009.v1.9

Saleh, N., Azis, N., Jasni, J., Kadir, M. Z. A. A., & Talib, M. A. (2021). Prediction of a transformer's loading and ambient temperature based on SARIMA approach for hot-spot temperature and loss-of-life analyses. In *IEEE International Conference on the Properties and Applications of Dielectric Materials (ICPADM)* (pp. 123-126). IEEE Publishing. https://doi.org/10.1109/ICPADM49635.2021.9493865

Saleh, N., Azis, N., Jasni, J., Kadir, M. Z. A. A., & Talib, M. A. (2022). Paper lifetime mathematical modelling based on multi pre-exponential factors for oil-immersed transformer. *Pertanika Journal of Science and Technology, 30*(2), 1115-1133. https://doi.org/10.47836/pjst.30.2.15

Sinha, A., Tayal, R., Vyas, A., Pandey, P., & Vyas, O. P. (2021). Forecasting electricity load with hybrid scalable model based on stacked non linear residual approach. *Frontiers in Energy Research, 9*, 1-17. https://doi.org/10.3389/fenrg.2021.720406

Susa, D., Lehtonen, M., & Nordman, H. (2005a). Dynamic thermal modeling of distribution transformers. *IEEE Transactions on Power Delivery, 20*(3), 1919-1929. https://doi.org/10.1109/TPWRD.2005.848675

Susa, D., Lehtonen, M., & Nordman, H. (2005b). Dynamic thermal modelling of power transformers. *IEEE Transactions on Power Delivery, 20*(1), 197-204. https://doi.org/10.1109/TPWRD.2004.835255

Teymouri, A., & Vahidi, B. (2019). Estimation of power transformer remaining life from activation energy and pre-exponential factor in the Arrhenius equation. *Cellulose, 26*, 9709-9720. https://doi.org/10.1007/s10570-019-02746-w

Tripathy, D. S., & Prusty, B. R. (2021). Quantile regression averaging-based probabilistic forecasting of daily ambient temperature. *International Journal of Numerical Modelling: Electronic Networks, Devices and Fields, 34*(3), 1-19. https://doi.org/10.1002/jnm.2846

Van den Berg, A. P. B., Bootsma, L. R., Bovenber, T. F. A., Moerbeek, A. R., De Jong, E., Khalil, S., Koch, T., & Dugundji, E. R. (2022). Year-ahead ambient temperature forecasting in pharmaceutical transport lanes thermal conditions. *Procedia Computer Science, 201*, 255-264. https://doi.org/10.1016/j.procs.2022.03.035

Zhang, E., Zheng, H., Zhang, C., Wang, J., Shi, K., Guo, J., Schwarz, H., & Zhang, C. (2021). Aging state assessment of transformer cellulosic paper insulation using multivariate chemical indicators. *Cellulose, 28*. https://doi.org/10.1007/s10570-021-03683-3